18

The Butterfly Gyro

Dag Billger

The Imego Institute
Arvid Hedvalls Backe 4, SE-411 33
Göteborg, Sweden
dag.billger@imego.com

Summary. A benchmark for structural mechanics, related to modeling of a microgyroscope, is presented. It can be used to apply model reduction algorithms to a linear second-order problem.

18.1 Brief Project Overview

The Butterfly gyro is developed at the Imego Institute in an ongoing project with Saab Bofors Dynamics AB. The Butterfly is a vibrating micro-mechanical gyro that has sufficient theoretical performance characteristics to make it a promising candidate for use in inertial navigation applications. The goal of the current project is to develop a micro unit for inertial navigation that can be commercialized in the high-end segment of the rate sensor market. This project has reached the final stage of a three-year phase where the development and research efforts have ranged from model based signal processing, via electronics packaging to design and prototype manufacturing of the sensor element. The project has also included the manufacturing of an ASIC, named μSIC, that has been especially designed for the sensor (Figure 18.1).

The gyro chip consists of a three-layer silicon wafer stack, in which the middle layer contains the sensor element. The sensor consists of two wing pairs that are connected to a common frame by a set of beam elements (Figure 18.2 and 18.3); this is the reason the gyro is called the Butterfly. Since the structure is manufactured using an anisotropic wet-etch process, the connecting beams are slanted. This makes it possible to keep all electrodes, both for capacitive excitation and detection, confined to one layer beneath the two wing pairs. The excitation electrodes are the smaller dashed areas shown in Figure 18.2. The detection electrodes correspond to the four larger ones.

By applying DC-biased AC-voltages to the four pairs of small electrodes, the wings are forced to vibrate in anti-phase in the wafer plane. This is the excitation mode. As the structure rotates about the axis of sensitivity (Figure 18.2), each of the masses will be affected by a Coriolis acceleration. This

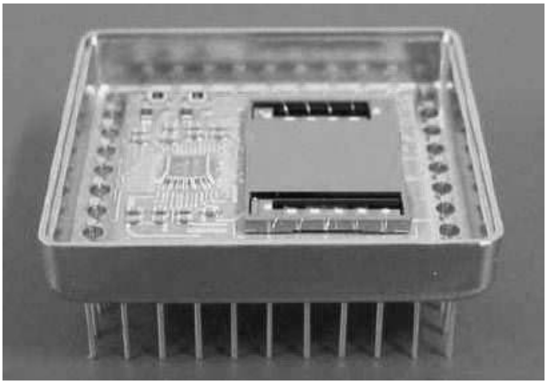

Fig. 18.1. The Butterfly and μSIC mounted together.

acceleration can be represented as an inertial force that is applied at right angles with the external angular velocity and the direction of motion of the mass. The Coriolis force induces an anti-phase motion of the wings out of the wafer plane. This is the detection mode. The external angular velocity can be related to the amplitude of the detection mode, which is measured via the large electrodes.

The partial differential equation for the displacement field of the gyro is governed by the standard linear equations of three-dimensional elastodynamics:

$$\sigma_{ij,j} + f_i = \rho \ddot{u}_i, \tag{18.1}$$

where ρ is the mass density, σ_{ij} is the stress tensor, f_i represents external loads (such as Coulomb forces) and u_i are the components of the displacement field. The constitutive stress-strain relation of a linear, anisotropic solid is given by

$$\sigma_{ij} = \frac{1}{2} C_{ijkl} \left(u_{i,j} + u_{j,i} \right), \tag{18.2}$$

where C_{ijkl} is the elastic moduli tensor.

18.2 The Benefits of Model Order Reduction

When planning for and making decisions on future improvements of the Butterfly, it is of importance to improve the efficiency of the gyro simulations. Repeated analyses of the sensor structure have to be conducted with respect to a number of important issues. Examples of such are sensitivity to shock, linear and angular vibration sensitivity, reaction to large rates and/or acceleration, different types of excitation load cases and the effect of force-feedback.

The use of model order reduction indeed decreases runtimes for repeated simulations. Moreover, the reduction technique enables a transformation of

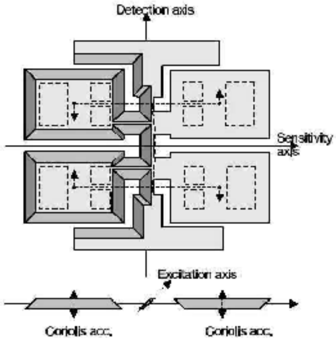

Fig. 18.2. Schematic layout of the Butterfly design.

the FE representation of the gyro into a state space equivalent formulation. This will prove helpful in testing the model based Kalman signal processing algorithms that are being designed for the Butterfly gyro.

The structural model of the gyroscope has been done in ANSYS using quadratic tetrahedral elements (SOLID187, Figure 18.3). The model shown is a simplified one with a coarse mesh as it is designed to test the model reduction approaches. It includes the pure structural mechanics problem only. The load vector is composed from time-varying nodal forces applied at the centers of the excitation electrodes (Figure 18.2). The amplitude and frequency of each force is equal to 0.055 μN and 2384 Hz, respectively. The Dirichlet boundary conditions have been applied to all DOFs of the nodes belonging to the top and bottom surfaces of the frame. The output nodes are listed in Table 18.2 and correspond to the centers of the detection electrodes.

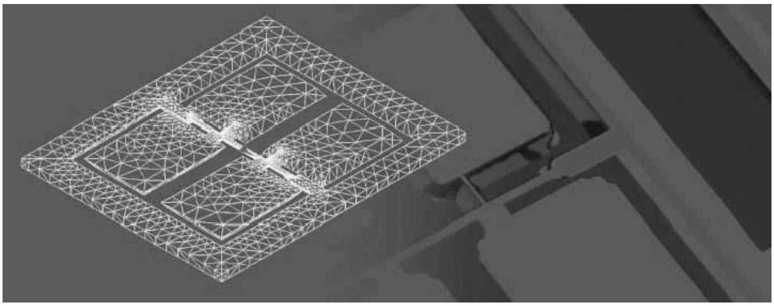

Fig. 18.3. Finite element mesh of the gyro with a background photo of the gyro wafer pre-bonding.

The discretized structural model

$$\begin{aligned} M\ddot{x} + E\dot{x} + Kx &= Bu \\ y &= Cx \end{aligned} \tag{18.3}$$

contains the mass and stiffness matrices. The damping matrix is modeled as $\alpha\mathbb{M} + \beta\mathbb{K}$, where the typical values are $\alpha = 0$ and $\beta = 10^{-6}$, respectively. The nature of the damping matrix is in reality more complex (squeeze film damping, thermo-elastic damping, etc.) but this simple approach has been chosen with respect to the model reduction benchmark.

The dynamic model has been converted to Matrix Market format by means of mor4ansys. The statistics for the matrices is shown in Table 18.1.

Table 18.1. System matrices for the gyroscope.

matrix	m	n	nnz	Is symmetric?
$\mathbb{M}$	17361	17361	178896	yes
$\mathbb{K}$	17361	17361	519260	yes
$\mathbb{B}$	17361	1	8	no
$\mathbb{C}$	12	17361	12	no

Table 18.2. Outputs for the Butterfly Gyro Model.

#	Code	Comment
1-3	det1m_Ux, det1m_Uy, det1m_Uz	Displ. of det. elect. 1, hardpoint #601
4-6	det1p_Ux, det1p_Uy, det1p_Uz	Displ. of det. elect. 2, hardpoint #602
7-9	det2m_Ux, det2m_Uy, det2m_Uz	Displ. of det. elect. 3, hardpoint #603
10-12	det2p_Ux, det2p_Uy, det2p_Uz	Displ. of det. elect. 4, hardpoint #604

The benchmark has been used in [LDR04] where the problem is also described in more detail.

References

[LDR04] Lienemann, J., Billger, D., Rudnyi, E.B., Greiner, A., Korvink, J.G.: MEMS Compact Modeling Meets Model Order Reduction: Examples of the Application of Arnoldi Methods to Microsystem Devices. In: The Technical Proceedings of the 2004 Nanotechnology Conference and Trade Show, Nanotech 2004, March 7-1, Boston, Massachusetts, USA, vol. 2, p. 303-306 (2004)